Microstructure and Phase Behavior of Block Copoly(ether ester) Thermoplastic Elastomers

Wouter Gabriëlse,* Maria Soliman, and Krijn Dijkstra

DSM Research, P.O. Box 18, 6160 MD Geleen, The Netherlands

Received July 20, 2000; Revised Manuscript Received December 22, 2000

ABSTRACT: The microstructure of segmented block copoly(ether esters) composed of poly(tetramethylene oxide) (PTMO) "soft" blocks and poly(butylene terephthalate) (PBT) "hard" blocks was investigated. A variety of analytical techniques, including ^{13}C solid-state NMR, infrared spectroscopy, dynamical mechanical analysis, dielectric spectroscopy, differential scanning calorimetry, and transmission electron microscopy, were applied. The samples vary in the amount (35−60 wt %) and block length (1000−2000 g/mol) of the soft component. It is generally assumed in the literature that copoly(ether esters) have a two-phase structure consisting of a crystalline PBT phase surrounded by an amorphous phase which is a homogeneous mixture of PTMO soft segments and amorphous PBT segments. Our experimental results reveal that the amorphous phase is not a homogeneous mixture of "hard" and "soft" segments but consists of a highly mobile "PTMO-rich phase" and a less mobile "PBT/PTMO mixed phase". The extent of microphase separation in the amorphous phase appeared to be strongly dependent on the block length and composition. Those samples that revealed a strong microphase separation showed strain-induced crystallization of the soft segments upon mechanical deformation.

1. Introduction

An industrially important class of thermoplastic elastomers (TPEs) are the segmented block copoly(ether esters).[1] DSM is one of the main mondial suppliers of these type of materials, which are marketed under the trade name Arnitel. These materials combine good low-temperature flexibility with an excellent mechanical and thermooxidative stability up to high temperatures and a good resistance against many chemicals. Therefore, this class of materials is frequently encountered in applications where severe demands are placed on stiffness and strength from low to high temperatures. Furthermore, these systems can be processed from the melt which enables product designs not easily achievable for conventional rubbers. In this paper we report on a well-known type of copoly(ether ester) composed of poly(tetramethylene oxide) (PTMO) "soft" segments and poly(butylene terephthalate) (PBT) "hard" segments.

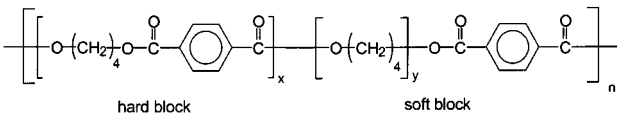

Since copoly(ether esters) form a heterogeneous structure by nature, understanding of morphology development is of great importance for understanding the physical properties of such materials. The TPE should have a rubber plateau which is as wide and as flat as possible and which has a level that is adjustable according to requirements of a certain application. All these parameters are sensitive to which phases are formed upon cooling from the melt and the way these phases are spatially arranged (for instance: disperse vs co-continuous). Important parameters in this respect are crystallinity, crystal perfection, composition of the amorphous phase, and continuity of the different phases.

* To whom correspondence should be addressed.

The phase behavior of copoly(ether esters) has been studied most extensively.[1] In the molten state, these systems typically form a homogeneous mixed phase of polyether and polyester segments. Upon cooling, at a certain temperature the polyester segments start to crystallize. There is evidence that crystallization starts from a homogeneous melt and that the crystallization process is the driving force for phase separation.[2−4] Upon further cooling to room temperature, a phase-separated structure is obtained consisting of PBT crystallites embedded in an amorphous matrix. The crystalline structure is typically lamellar.[5,6] Furthermore, a crystalline superstructure (spherulites) can be formed depending on the crystallization conditions.[7]

In general, the crystallization process and the structure of the crystalline phase have been studied in detail in the past. Much less attention was paid to the structure of the amorphous phase. Within the composition ranges studied, most authors conclude that after crystallization the copoly(ether ester) can be described by a two-phase model: a crystalline polyester phase and a homogeneous amorphous phase of the polyether mixed with the noncrystalline polyester.[1,7,8,9] Both phases are considered to be continuous.[8,10] Despite the general claim that a homogeneous amorphous phase is present, the glass transition as measured with a dynamical mechanical analysis is very broad and sometimes shows a shoulder.[5,11,12] In this study we investigated in more detail the structure of the amorphous phase, which has not been clarified in the present literature.[1−12] The implications of the microphase structure of the amorphous phase on the tensile behavior will also be discussed in this paper. A wide compositional range has been investigated in order to provide a more general understanding of the morphology of copoly(ether esters) instead of restricting the study to only a single composition. For this purpose we synthesized a series of copoly(ether esters) with a systematic variation in block length and composition. The phase behavior and microstructure of these model systems were characterized in detail

10.1021/ma0012696 CCC: $20.00
Published on Web 02/20/2001

Table 1. Composition and End-Group Concentrations of the Copoly(ether esters)

	model systems					
	1000/35	1000/50	1500/50	1000/60	1500/60	2000/60
composition [wt %]						
DMT	43.4	36.1	36.1	30.0	30.0	30.0
BDO	30.3	25.2	25.2	21.3	21.3	21.3
PTMO (1000 g/mol)	25.3	37.6		47.6		
PTMO (1500 g/mol)			37.6		47.6	
PTMO (2000 g/mol)						47.6
end-group concn [mequiv/kg]						
E_{OH}	42	60	53	47	47	67
E_{COOH}	36	27	20	27	35	18

by a number of experimental techniques including transmission electron microscopy (TEM), differential scanning calorimetry (DSC), dynamical mechanical analysis (DMTA), dielectric spectroscopy (DIES), and ^{13}C solid-state NMR. For the latter method, we made use of the ^{13}C inversion recovery cross-polarization (IRCP) technique,[13] which is very sensitive to differences in molecular mobility. The changes in phase behavior of the material under mechanical deformation was also studied using infrared spectroscopy. On the basis of the obtained results, a refined structural model is proposed, which provides a better understanding on the relations between molecular structure, microstructure, and mechanical properties.

2. Experimental Section

2.1. Model Systems. The copoly(ether esters) are synthesized by melt transesterfication and subsequently polycondensation of dimethyl terephthalate (DMT), 1,4-butanediol (BDO), and poly(tetramethylene oxide) (PTMO) with varying molecular weight. The catalyst used is tetrabutyl titanate (TBT), and the polyether is protected against oxidation during polymerization by 1,3,5-trimethyl-2,4,6-tris(3,5-di-*tert*-butyl-4-hydroxybenzyl)benzene. The compositions of the copolymers are given in Table 1. The polycondensation reaction is carried out at a temperature of 250 °C under vacuum, with a typical polymerization time of 200 min. Resulting end-group concentrations are also given in Table 1. After polymerization, the polymer is extruded as a strand and pelletized. The polymer granules are consequently dried at 100 °C for 2 h and at 140 °C for 5 h.

The model copoly(ether ester) compounds vary in the amount (35−60 wt %) and in the number-average molecular weight of the soft segments (1000−2000 g/mol). Table 1 summarizes the investigated model compounds. The samples are identified by the weight percent and molecular weight of the soft PTMO segments by a code such as 2000/60 (60 wt % PTMO of molecular weight 2000). The average PBT block length is directly determined by both parameters. It is noted that in our definition the terephthalic acid group at the transition of the polyester to the polyether is counted to the soft segment.[8] It was only possible to synthesize those materials given in Table 1. Other compositions will show macrophase separation during polymerization,[1] which results in a block copolymer with a broad distribution in composition and inferior mechanical properties. The melt homogeneity of the investigated samples was assessed by visual inspectation, which is sufficient to confirm the absence of macrophase separation. The total molecular weight M_n of the samples is approximately 25 000 g/mol. The M_w/M_n ratio for PTMO and PBT is 2.4 and 2, respectively. The sequence distribution was not characterized for our samples. Recently, sequence distributions for PBT/PTMO block copoly(ether esters) were determined by Min et al.[14] by NMR spectroscopy. Those systems were synthesized in a similar way as ours. Therefore, we expect that the sequence distributions for our samples have comparable triad probabilities. More details can be found in this reference. All samples were injection-molded into the form of plates. On the basis of relative viscosity measurements, no significant effects of molding on the molecular weight of the samples could be observed.

2.2. Characterization Methods. Transmission electron micrographs were obtained using a Philips CM200 electron microscope. The samples were stained for 48 h with a 1:1 mixture of a 2% aqueous solution of OsO_4 and a 20% aqueous solution of formaldehyde.

The thermal characteristics of the polymers were measured with a Perkin-Elmer DSC-7 apparatus using a heating and cooling rate of 10 °C/min. The temperature ranged between −100 and 250 °C. Dynamical mechanical measurements were performed with a RSA2 (Rheometrics) with constant frequency (1 Hz). The samples were first cooled to −130 °C and subsequently heated to 200 °C at a heating rate of 5 °C/min. Dielectric measurements were performed on a home-built apparatus. Temperature scans were performed in the range from −150 to 70 °C at several frequencies in the range from 125 mHz to 1 MHz. The heating or cooling rate was 10 °C/min. The samples were 4 mm thick.

^{13}C solid-state nuclear magnetic resonance experiments were carried out at a Varian Unity 400 (400 MHz for ^1H) spectrometer using a 7 mm VT CP/MAS probe. All NMR experiments were performed at room temperature. The 90° pulse width was 5 μs for protons and carbons. Adamantane was used as an external chemical shift reference (38.3 ppm for the methylene resonance relative to TMS). All experiments were performed under magic angle spinning (spinning rate = 4 kHz) and high-power decoupling conditions (50 kHz field strength). A recycle time of 2 s was used in all cross-polarization experiments. ^{13}C inversion recovery cross-polarization (IRCP) experiments[13] were performed by applying a 180° phase shift on the proton spin-locking field. The cross-polarization time τ_1 was set to a fixed value of 1 ms. The "inversion time" τ_2 was varied between 0.005 and 20 ms. The $180°-\tau-90°-T_1$ inversion recovery pulse sequence was used to obtain quantitative ^{13}C spectra. For the analysis of the NMR spectra, a self-written peak deconvolution program was used. Infrared spectra were recorded with a Bruker rapid scan spectrometer that was connected to a home-built tensile machine. Dichroism measurements were performed during a tensile test. For each spectrum, 43 scans were accumulated, and each spectrum took 10 s to be completed. Each measurement resulted in 60 spectra, 30 spectra in the strain direction (parallel), and 30 spectra in the direction perpendicular to the strain direction.

3. Results and Discussion

3.1. Transmission Electron Microscopy. Well-developed spherulitic structures with a diameter of ca. 5−20 μm were clearly observed using a polarized light microscope (not shown here). The morphology at a nanometer scale was investigated using transmission electron microscopy. As an example, transmission electron micrographs of samples 1500/60 and 1000/35 are shown in Figure 1. The soft domains are considered to absorb the staining agent and are visible as black regions; the crystalline domains appear as white regions. The transmission electron micrographs clearly indicate that copoly(ether esters) possess at least a two-

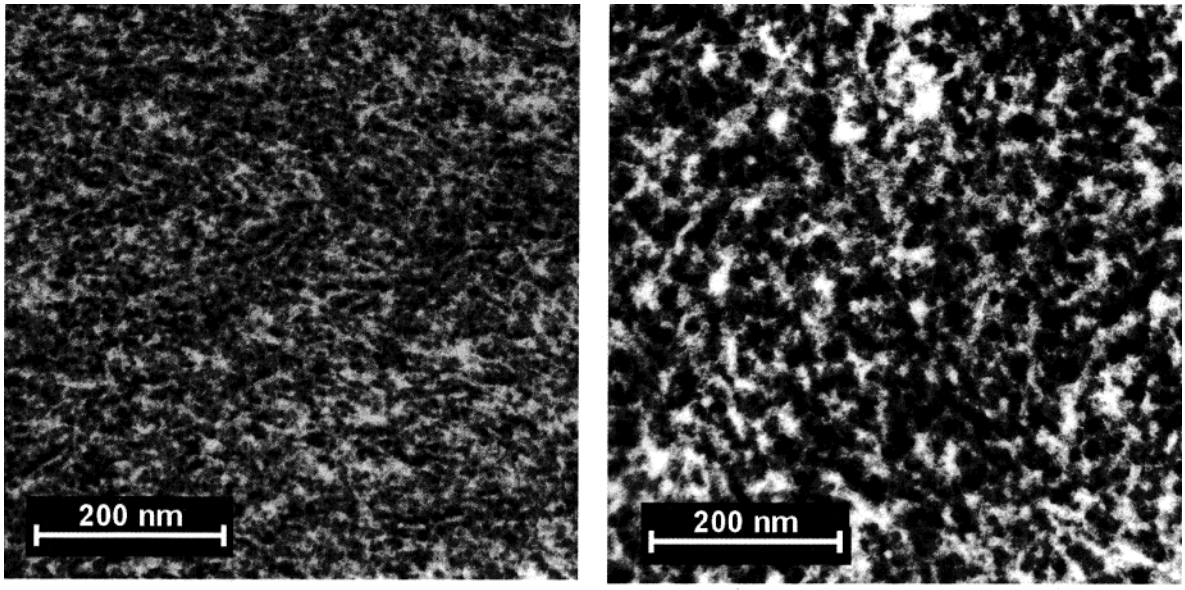

Figure 1. Transmission electron micrographs of sample 1000/35 (a) and 1500/60 (b).

Table 2. Transition Temperatures for the Model Copoly(ether esters) Obtained from Various Techniques

sample	T_g(DSC) [°C]	T_g^1(DMTA) [°C]	T_g^2(DMTA) [°C]	T_g^1(DIES) (0.5 Hz) [°C]	T_g^2(DIES) (0.5 Hz) [°C]	T_m^{PTMO}(DSC) [°C]	T_m^{PBT}(DSC) [°C]
1000/35	−43	−42	*a*	−38	*a*	*a*	209
1000/50	−64	−62	*a*	−62	*a*	*a*	188
1500/50	−72	−71	−27	−72	−22	−2	202
1000/60	−67	−65	−35	−70	−28	−15	157
1500/60	−70	−70	−23	−72	−25	−5	175
2000/60	−73	−70	−20	−74	−20	0	194

[a] No detectable transition.

Table 3. Various Structural Parameters of the Model Copoly(ether esters)

sample	E'(25°) [MPa] DMTA	domain size amorphous phase (TEM) [nm]	P_n (PBT)[a]	$w_{C,PBT}$ [b]	$w_{C,sample}$ [c]	fraction PTMO in "PTMO-rich phase" (^{13}C NMR)	ϵ_{cryst} [d] (%) (IR)
1000/35	250	10	9	0.44	0.32	0.28	
1000/50	100	15	5	0.50	0.22	0.44	
1500/50	70	20	7.5	0.44	0.22	0.61	160
1000/60	36	18	3	0.31	0.13	0.64	320
1500/60	45	26	5	0.42	0.17	0.62	220
2000/60	48	33	6.5	0.41	0.17	0.76	100

[a] Average number of PBT monomer repeat units as calculated from the average block length and concentration of soft PTMO segments. [b] PBT crystalline weight fraction determined from melting enthalpy of perfect crystalline PBT (ΔH_m^0 = 145.5 J/g).[15] [c] Total sample weight fraction crystallinity. [d] Strain onset values for strain-induced crystallization of PTMO at room temperature as detected with IR.

phase morphology. Similar micrographs of copoly(ether esters) have been reported in the literature.[8] We observed small variations in the morphology for the model systems. Especially for the materials with relatively short soft block lengths and a low weight percent of soft segments, i.e., longer PBT blocks (larger than approximately five monomer units), lamellar crystalline structures are visible (see Figure 1a). Sample 1500/60 shows a more coarse structure compared to sample 1000/35 with larger dimensions of crystalline and amorphous domains. The domain sizes of the amorphous phase seem to increase with the concentration and block length of the soft segments. Typical domain sizes of approximately 10−30 nm for the soft phase were determined (see Table 3).

3.2. Differential Scanning Calorimetry. The thermal behavior of the polymers is illustrated in Figure 2 for two samples: sample 1500/60 and 1000/35. Obviously, there are clear differences for both samples. For sample 1500/60 the thermogram reveals a clear glass transition at about −70 °C. The glass transition is higher than that of pure PTMO, which has a T_g of −90 °C.[12] The rise of T_g of the soft phase in the copolymer is caused by chemical linkage to the rigid crystalline PBT blocks and partial mixing with amorphous PBT hard segments. Furthermore, two melting endotherms are observed. The first melting endotherm has a maximum at −2 °C and is attributed to melting of PTMO crystallites. The second melting endotherm, which is rather broad and has a maximum at 177 °C, is attributed to melting of PBT crystallites. For sample 1000/35 we observe a relatively broad glass transition ($T_g \sim -43$ °C) and only one melting peak (T_m = 208 °C) in the high-temperature region of PBT. In neither one of the

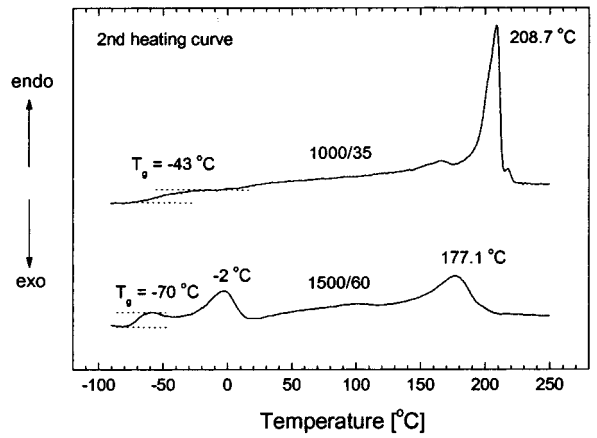

Figure 2. DSC curves of sample 1000/35 and sample 1500/60.

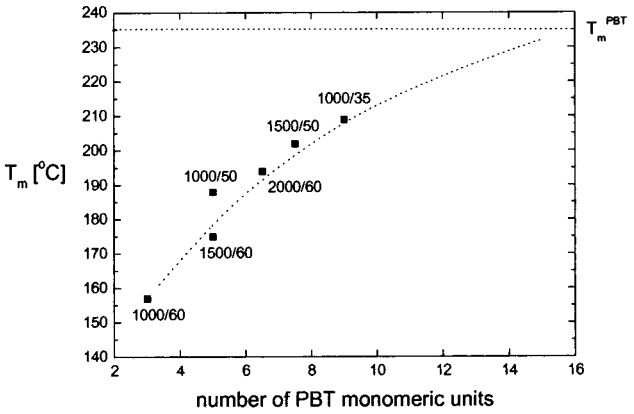

Figure 3. Melting point (T_m) for the various model copoly(ether esters) vs average PBT block length. The dotted line is not a curve fit but is a guide to the eye.

samples a glass transition of PBT, which should appear around 50 °C, could be observed in the DSC traces.

The melting endotherm of PTMO in the vicinity of 0 °C is found only for samples with a relatively large concentration PTMO and/or long PTMO block length, i.e., samples 2000/60, 1500/60, 1000/60, and 1500/60. The maxima in these curves, i.e., melting points, lie between −15 and 0 °C (see Table 2). For both the PBT and PTMO crystallites, the melting temperature is lower than that of the homopolymers ($T_m^{PTMO} \sim 35$ °C; $T_m^{PBT} \sim 230$ °C).[15] The decrease of the melting temperature in the copolymers is attributed to the limited crystallite size and to the larger amount of crystal imperfections due to the less favorable crystallization conditions compared to the homopolymers. For the model systems studied here the melting point of PBT varies between 157 and 209 °C. It appears that the melting point of the PBT crystallites increases with increasing the average block length of PBT segments, as is graphically illustrated in Figure 3. Upon extrapolation to longer PBT block lengths, the melting point of the PBT homopolymer is approached. The average PBT block length was calculated directly from the known polymer composition and average block length of the soft blocks. These results, which are consistent with results reported in the literature,[1] suggest that the crystallite size and crystallite perfection increase with increasing block length.

The weight fraction of hard segments that are incorporated in the crystals ($w_{C,PBT}$) can be determined from

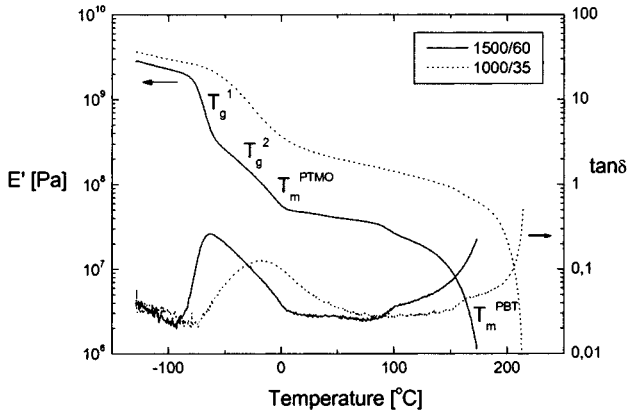

Figure 4. Dynamical mechanical data of sample 1000/35 and 1500/60.

the enthalpy of melting, assuming a melting enthalpy of 145.5 J/g for perfect crystalline PBT.[15] These values are given in Table 3. The $w_{C,PBT}$ values vary between 0.31 and 0.50, which is in agreement with values reported in the literature.[12] Also, the total weight fraction of crystalline material in the sample ($w_{C,total}$) is given in Table 3. These values range from 0.13 to 0.32. It appears that the PBT crystallinity is almost independent of the composition and the average PBT block length, with the exception of sample 1000/60 which shows a lower PBT crystallinity of 0.31. It is noted that the latter sample contains PBT segments with a rather short average block length of three units. These results indicate that a substantial amount of PBT segments (at least 50 wt %) must be located in the amorphous phase. It is likely that those sequences shorter than the average block length do not take part in the crystallization process and are rejected into the amorphous phase.

3.3. Dynamic Mechanical Measurements. Dynamic mechanical measurements can provide a good impression of the phase behavior of these co-poly(ether esters).[1,11,12] In general, it is stated in the literature that copoly(ether esters) exhibit only one glass transition, as indicated by differential scanning calorimetric and dynamical mechanical data.[1,11,12] Still, dynamical mechanical studies on similar model systems as studied by Seymour et al.[11] and Wegner et al.[12] do not show a single smooth glass transition but showed in some cases a more complex behavior. However, in none of these studies it was tried to elucidate these effects, and the amorphous phase has been treated as a single phase, which is a homogeneous mixture of hard and soft segments. Since we are interested in the structure of the amorphous phase, we investigated the glass transition region in more detail.

In Figure 4 , the E' curves and the tan(δ) curves of two model systems are shown (1500/60 and 1000/35). In general, three relaxation regions in E' can be distinguished. First a broad glass transition is observed in the temperature region between −80 and 0 °C. Above the glass transition region a rubber plateau is observed which is typical for elastomeric materials. Subsequently, at elevated temperatures (>∼100 °C) melting and recrystallization processes of less perfect PBT lamellae take place. (The material is quenched during injection molding, so there is no optimized crystalline structure present.) Finally, at the high-temperature end, complete melting of the PBT lamellae takes place which results in a fast drop in E modulus. Similar to the DSC

experiments, the DMTA curves for sample 1000/35 and 1500/60 show clear differences.

For sample 1500/60, we can clearly observe three steps in the temperature region between −80 and 0 °C. In addition, an asymmetric maximum is observed in the tan(δ) curve. The loss in E' in the temperature region between −20 and 0 °C can unambiguously be assigned to melting of PTMO crystals as was already revealed by DSC measurements (see previous paragraph). The two other steps are considered to be two glass transitions, which indicates the presence of two distinct amorphous phases, which differ in composition. We are aware that this interpretation is preliminary, but our interpretation is strongly supported by the ^{13}C solid-state NMR results (discussed later). According to the NMR results, the amorphous phase with the low T_g is rich in PTMO segments, whereas the amorphous phase with the higher T_g contains a substantial fraction of amorphous PBT mixed with PTMO. Hence, the lower T_g, T_g^1, at about −70 °C is attributed to an amorphous phase rich in soft segments (PTMO-rich) and the higher T_g, T_g^2, which appears at about −25 °C is attributed to a mixed amorphous phase (PBT/PTMO mixed) which contains both hard and soft segments.

For sample 1000/35 a single glass transition is observed, with a T_g at about −40 °C, which is in between that of the pure components (−90 °C for PTMO and ca. 50 °C of PBT).[12] The broad glass transition is attributed to a broad compositional distribution of mixed phases of hard and soft segments. A melting transition of PTMO crystals, which should appear at ca. 0 °C, cannot be observed for this sample. Except for the samples 1000/35 and 1000/50, for all other model materials, two distinct glass transitions could be observed. The glass transition temperatures are given in Table 2. In neither one of the samples, a glass transition of a pure amorphous PBT phase at ca. 50 °C or lower was observed.

3.4. Dielectric Investigations. The results of the dielectric measurements of compounds 1000/35 and 1500/60 are shown in Figure 5 as a function of temperature for eight selected frequencies (0.5 Hz−1 MHz). For both materials a secondary relaxation peak in the dielectric constant can be seen between ca. −150 and −80 °C, which is related to local ether rotation of the soft segments. Similar to the DMTA results, sample 1500/60 shows distinct transitions in the dielectric constant as a function of temperature, especially at low frequencies. First, a sharp increase in ϵ' can be seen at ca. −70 °C, which is followed by a gradual increase in ϵ' between −70 and 0 °C. Around 0 °C an almost frequency-independent maximum is observed, which is attributed to melting of PTMO crystals, as was observed with DSC. Above this temperature an increase of the dielectric constant for low frequencies can be seen (interfacial polarization phenomena) and a constant decrease of the high-frequency values (expected temperature dependence above T_g). Following the interpretation of the DMTA results, the sharp transition at ca. −70 °C and the broad transition between −70 and 0 °C are attributed to two glass transitions: one of a phase rich in soft segments (T_g^1) and one related to a phase with substantial mixing of hard and soft segments (T_g^2). It should be noted that pure PBT shows a secondary relaxation at −40 °C. It consists of a combination of several local main chain relaxations. However, this relaxation is very broad and is much less intense than the relaxation processes of the soft segments in the copoly(ether ester). Therefore, it is assumed that the contribution of the PBT relaxation process to the relaxation process of the copoly(ether ester) in this temperature range is not significant. From the dielectric measurement it is difficult to assign clear transition temperatures to the steps occurring in ϵ'. The T_g's which are given in Table 2 are determined from the low-frequency curve (0.5 Hz). The observation of two glass transitions for sample 1500/60 can also be seen in the dielectric loss curve: especially at low frequencies an asymmetric loss peak is found similar to the tan(δ) curve in DMTA. At higher frequencies it splits up into two maxima, which is most clearly seen in the 10 kHz curve (see Figure 5c). It is noted that the T_g's as measured with DIES correspond well with the T_g's as determined with DMTA (see Table 2).

For sample 1000/35 we only observe a broad glass transition region in ϵ' (only a single step) and ϵ'' (a relatively broad symmetric peak). As was mentioned before, no melting of PTMO is observed for this sample. These results are consistent with the DSC and DMTA results as discussed before.

Consistent with DMTA measurements, for samples with a relatively long block length and larger weight fraction of soft segments, two steps in the dielectric constant in the glass transition region were visible. Samples 1000/50 and 1000/35 showed only one broad glass transition.

3.5. Solid-State NMR. Solid-state NMR is a powerful tool for investigating the microphase structure of polymers at a nanometer scale. Especially NMR relaxation studies are of interest, since changes in morphology are usually accompanied by changes in molecular mobility which are reflected in NMR relaxation times. Recently, NMR relaxation studies on these types of copoly(ether esters) were reported by Schmidt et al.[16] On the basis of $T_{1\rho}$ experiments on protons and carbons, they suggested a microphase separation in the amorphous phase. We will provide clear evidence for this phenomenon by using a ^{13}C inversion recovery cross-polarization (IRCP) experiment.

A ^{13}C solid-state CP-MAS spectrum of a copoly(ether ester) based on PBT and PTMO is shown in Figure 6. Spinning sidebands that appear due to fast rotation of the sample are marked with an asterisk. The assignments are indicated in the figure: carbonyl resonances of PBT are observed at 165 ppm (e), the aromatic resonances of PBT at 130 (g) and 134 ppm (f). The methylene CH_2 resonances of PBT and PTMO (a, d) overlap and give a single peak at 27 ppm. The OCH_2 resonances of PTMO and PBT are observed separately at respectively 71 (c) and 65 ppm (b). In this study we are interested in the mobility of the soft phase, so we concentrated on the resonance at 71 ppm, which belongs to the OCH_2 carbons of PTMO.[17]

The ^{13}C IRCP pulse sequence is shown in Figure 7a. The experiment is composed of two contiguous parts.[13] The first step is a classical cross-polarization step, during which magnetization is transferred from the abundant ^1H spins to the dilute ^{13}C spins for a contact time τ_1. During the second part of the experiment (τ_2), the carbon magnetization is inverted. The rate of this inversion process or depolarization process is determined by the cross-polarization dynamics. The cross-polarization or depolarization rate depends on the strength of the magnetic dipole−dipole coupling between ^{13}C and ^1H spins, which is affected by molecular

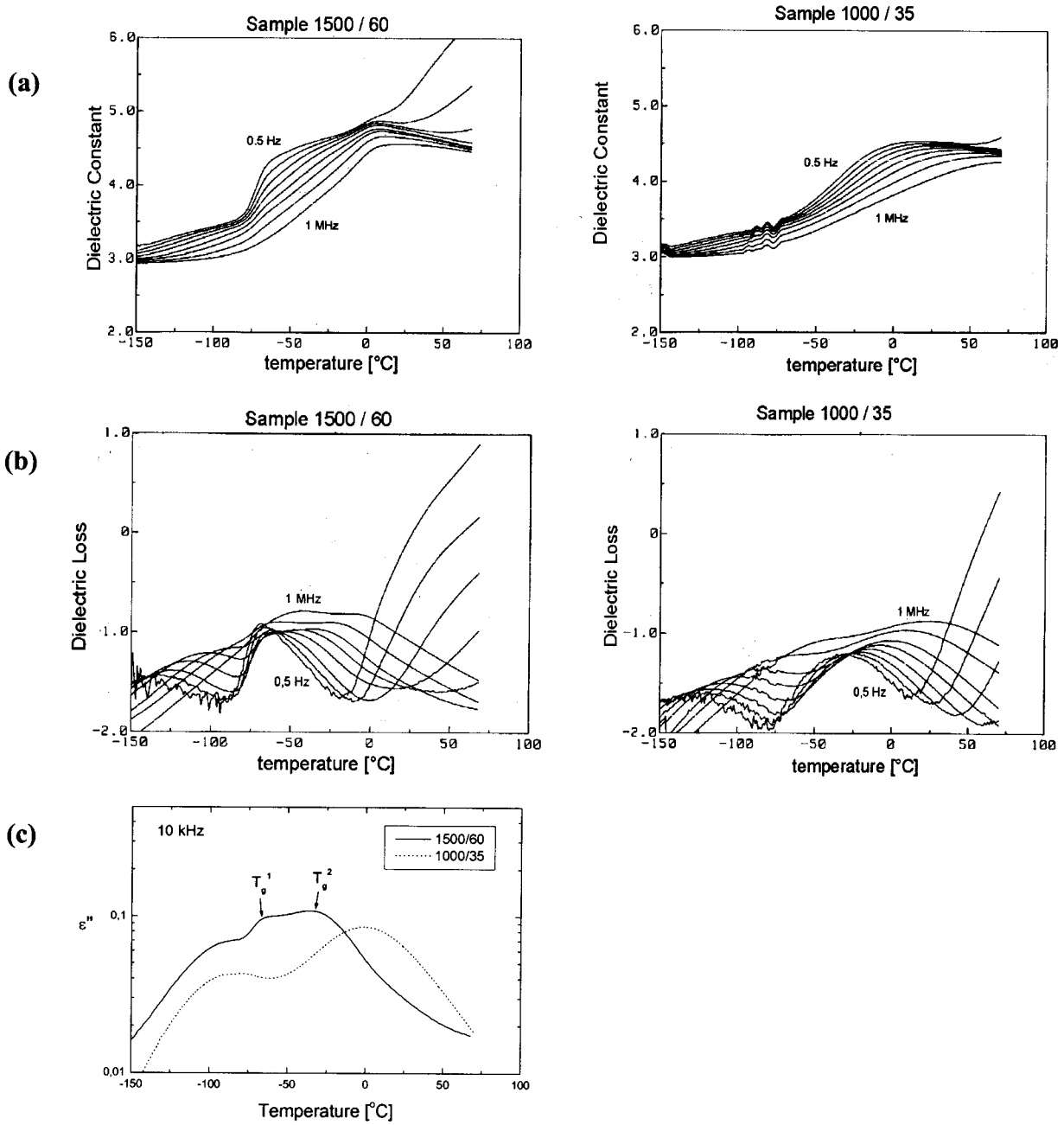

Figure 5. Dielectric constant (a) and dielectric loss (b) at various frequencies (0.5 Hz, 2 Hz, 16 Hz, 128 Hz, 1 kHz, 10 kHz, 100 kHz, and 1 MHz) as a function of temperature for samples 1500/60 and 1000/35; (c) dielectric loss of sample 1500/60 and 1000/35 at 10 kHz as a function of temperature.

motions. In the case of slow motions or low-amplitude motions cross-polarization is a relatively fast process; in the case of fast motions or high-amplitude motions, cross-polarization is a relatively slow process. This inversion process is illustrated in Figure 7b for a "hard" and a "soft" phase, which shows that the hard phase inverts faster than the soft phase. As a result, the "crossover" or "inversion point" will be different for both phases, which allows selective observation of one component by nulling the other.

The results of this experiment are shown in a stack plot in Figure 8 for sample 1000/60. The spectra recorded at different inversion times τ_2 are shown together with individual lines that compose these spectra. The spectra are not shown in absolute intensity mode but are scaled arbitrarily. Only the OCH_2 resonances of PTMO (71 ppm) and PBT (65 ppm) are shown. For the moment, the behavior of the OCH_2 resonances of PBT is not discussed. The spectrum at the "crossover" point at $\tau_2 = 600$ μs is of special interest. This spectrum clearly shows that the PTMO−OCH_2 resonance at 71 ppm, which appears as a single unresolved line in a ^{13}C CP/MAS spectrum, is actually composed of *two* resonances: a narrow peak (red) which is still positive and not yet inverted and a broader peak (blue) which has already been inverted. The narrow peak is shifted slightly upfield (~0.1 ppm) with respect to the broad line. We find for all samples that the OCH_2 resonance of PTMO at 71 ppm is composed of two resonances. By choosing appropriate inversion times τ_2, both peaks are observed separately. At $\tau_2 = 200$ μs, only the narrow peak is observed, whereas at $\tau_2 = 1200$ μs we only observe the broad peak. Consequently, we are able to estimate directly the peak parameters (peak position,

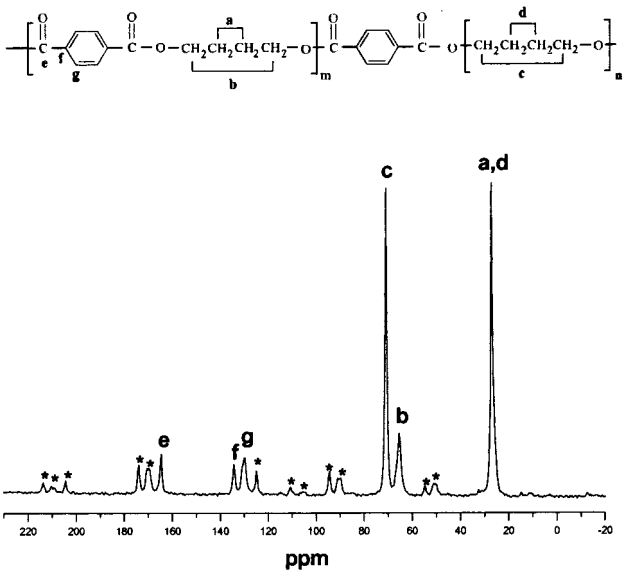

Figure 6. ^{13}C CPMAS spectrum of a copolyether ester (sample 1000/60). Assignments are indicated in the plot. Spinning sidebands are markes with an asterisk.

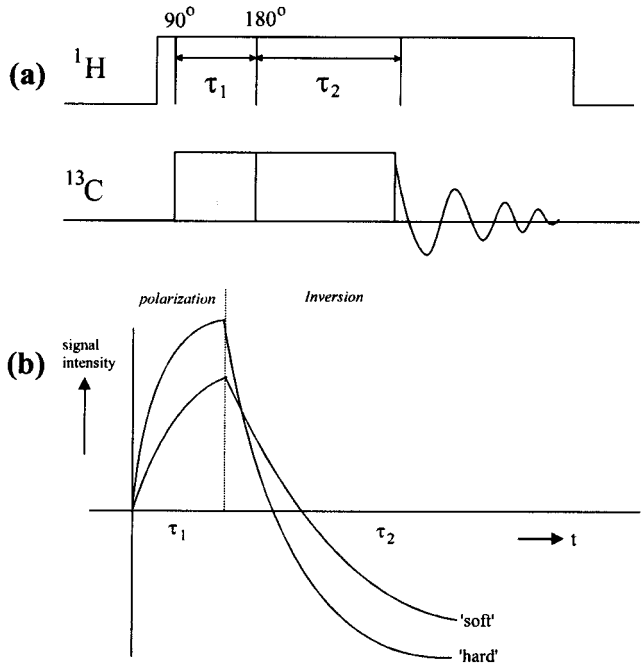

Figure 7. (a) Pulse sequence of the ^{13}C inversion recovery cross polarization (IRCP) experiment. (b) Schematic illustration of the development of ^{13}C signal intensity of a "hard" and "soft" phase.

peak width, and peak shape) of the narrow and broad lines without spectral deconvolution. These parameters were set to fixed values when fitting the quantitative ^{13}C spectra.

Obviously both resonances with different line width and cross-polarization behavior are related to PTMO segments with different mobility: the broad line can unambiguously be assigned to PTMO segments with more restricted mobility and the narrow line to highly mobile PTMO segments. These results strongly support the previously suggested model that the amorphous phase is not a homogeneous mixture of hard and soft segment but is composed of at least two distinct phases with a different composition: a highly mobile PTMO-rich phase and a less mobile PBT/PTMO mixed phase,

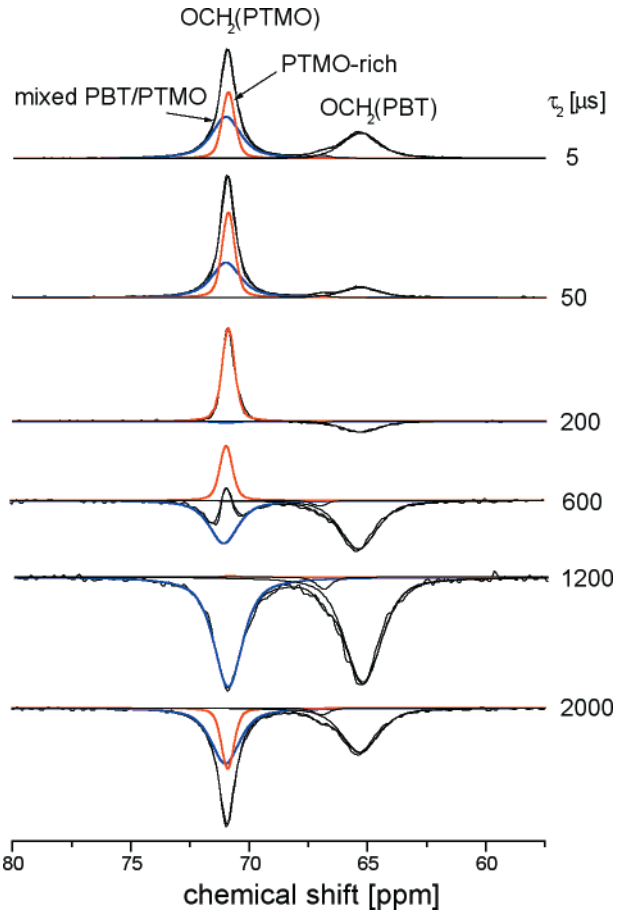

Figure 8. Deconvoluted ^{13}C IRCP spectra recorded at different inversion times τ_2 for sample 1000/60.

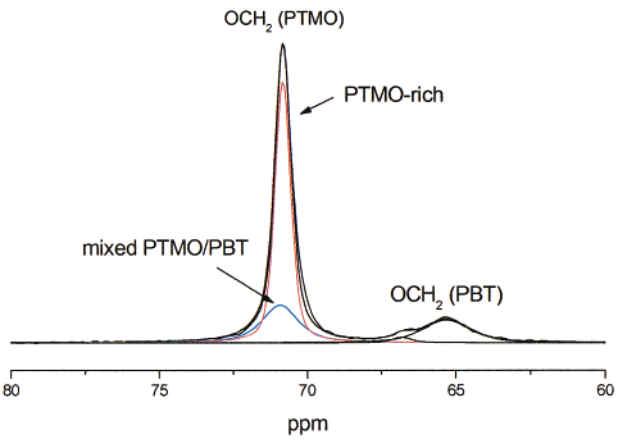

Figure 9. Quantitative ^{13}C NMR spectrum of sample 1000/60 showing the relative intensities of the PTMO-rich and mixed PBT/PTMO phase.

where the mobility of PTMO segments is more hindered due to the presence of PBT segments.

The fraction of PTMO segments that reside in both phases can be estimated from the corresponding peak areas of each line in a quantitative ^{13}C NMR spectrum. It appears that the ^{13}C T_1 relaxation time for PTMO−OCH_2 carbons is on the order of 0.5−1 s at room temperature, which means that a recycle delay of approximately 5 s is sufficient to record quantitative spectra. An example of a deconvoluted ^{13}C OCH_2 resonance of PTMO, recorded under quantitative conditions, is given in Figure 9. From the integrated peak areas, the fraction of PTMO in the PTMO-rich phase

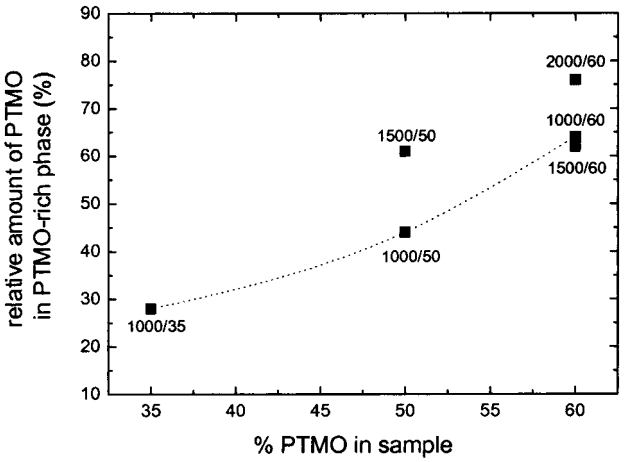

Figure 10. Fraction of PTMO soft segments in the PTMO-rich phase as determined from ^{13}C NMR as a function of the total amount of PTMO in the sample. The dotted line does not represent a curve fit but shows the trend in phase composition of the samples with the same PTMO block length of 1000 g/mol.

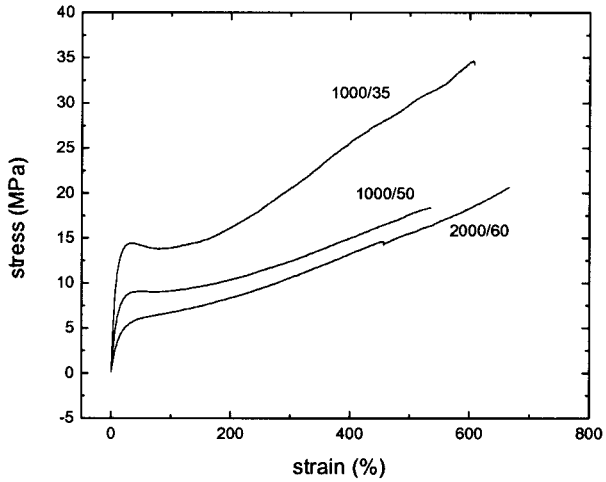

Figure 11. Stress−strain behavior of various copoly(ether ester) model compounds.

and in the amorphous PBT/PTMO mixed phase can be determined. These values are listed in Table 3. The error in these data is estimated to be less than 10%. The effect of block length and composition on the phase behavior of these systems is graphically illustrated in Figure 10. Obviously the phase behavior is strongly influenced by the composition of the system and to less extent by the block length of the soft blocks. The effect of composition is most clearly visible for the samples with a PTMO block length of 1000 g/mol (see dashed line). It is shown that the relative amount of PTMO that resides in the PTMO-rich phase increases significantly with increasing concentration of PTMO in the sample. Although we have only a limited number of data points, this effect seems to be less pronounced for samples with longer PTMO block lengths. Although less evident, a longer block length of PTMO seems to enhance the microphase separation in the amorphous phase. Summarizing, our NMR results indicate that the microphase separation in the amorphous phase is most pronounced in samples with a large concentration PTMO and long PTMO block length. This is consistent with DMTA and DIES results, which show two distinct T_g's for those samples. However, for samples 1000/35 and 1000/50, only one single broad glass transition was observed. Here we should realize that solid-state NMR compared to DMTA probes different length scales. The NMR measurements discussed here are sensitive to local segmental motions, whereas transitions in a DMTA curve involve motions where more segments are involved. In other words, the solid-state NMR measurements are able to detect microscopic heterogeneities on a much smaller scale than for instance DMTA, which makes it a very attractive technique for investigating the microphase structure on a subnanometer level.

3.6. Effect on Deformation Behavior. Finally we like to discuss the effect of the microphase separation in the amorphous phase on the deformation behavior. Typical stress strain curves are shown for samples 2000/60, 1000/50, and 1000/35 in Figure 11. The deformation behavior is typical for thermoplastic elastomers.[1] A linear behavior is observed for small deformations; then the slope changes (yielding) without strain softening. For sample 2000/60 a homogeneous deformation is observed up to large strains of ca. 700%. For sample 1000/35 a global necking behavior can be observed. At larger strains above ca. 200−300% strain hardening occurs until fracture. For sample 1000/50 only a minor necking behavior is observed.

The molecular deformation behavior was studied in more detail using infrared spectroscopy. An extended ^{13}C solid-state NMR study was reported before.[16] It is well-known from the literature that the PBT blocks undergo a reversible crystal transition between the α and the β structure by mechanical deformation.[18] This phenomenon was not studied in large detail for our samples; instead, we focused more on the deformation behavior of the amorphous phase. It was shown by ^{13}C solid-state NMR that above a certain strain level crystallization of the soft segments occurs.[16] It appeared that this transition is irreversible: the PTMO crystallites remain present when the mechanical stress is released. We observed the same effect with infrared measurements on stretched samples, where an absorption peak at 997 cm^{-1}, which was assigned to crystalline PTMO,[19] appears. By performing IR measurements continuously during a tensile test, the onset of strain-induced crystallization could be studied for each sample. These values are also listed in Table 3. It appears that only the soft materials with either long soft blocks or a large amount of PTMO show strain-induced crystallization. It can be clearly seen that for the samples with 60% PTMO the threshold strain values increase with decreasing block length. By performing infrared dichroism measurements, it was shown that the formed PTMO crystals were highly oriented along the stretching direction, which indicates that the formation of the crystals at room temperature, which is about 40 deg above the crystallization temperature, is preceded by alignment of neighboring PTMO segments along the stretching direction.

The deformation results fit well with our observation of microphase separation in the amorphous phase. Only for materials that show a good microphase separation, i.e., containing a relatively large amount of PTMO-rich phase, crystallization of PTMO upon mechanical deformation occurs. These results are in agreement with the ^{13}C NMR results of Schmidt et al.[16] This explains why PTMO crystallization is not observed for sample 1000/35 and 1000/50: a substantial amount of PTMO-rich phase must be present to allow crystallization upon mechanical deformation. In fact, the same samples that

show strain-induced crystallization of PTMO also showed a melting peak of PTMO in a DSC experiment. It is further noted that the strain-induced crystallization of PTMO does not lead to a significant increase in the stress level at the onset of crystallization as can be seen from Figure 11. This is probably caused by the gradual increase in PTMO crystallinity as a function of the applied strain, which has been observed in the infrared measurements.

4. Conclusions

Six model copoly(ether esters) were studied to determine their microstructure and phase behavior. A structural model composed of the following phases is proposed: (1) a crystalline PBT phase, where the small PBT crystallites act as physical cross-links between the amorphous soft segments, (2) a PBT/PTMO mixed amorphous phase, (3) a rubbery PTMO-rich phase, and (4) a crystalline PTMO phase which can be formed by cooling the sample below the T_m of PTMO or by mechanical deformation above a certain strain level. On the basis of our experiments, there was no clear evidence for the existence of a pure amorphous PBT phase. No T_g of amorphous PBT (around 50 °C) could be observed, neither in DSC nor in DMTA measurements.

Contrary of what is proposed in the literature, our investigations indicate that the amorphous phase of copoly(ether esters) cannot be considered as a homogeneous mixture of soft segments and uncrystallized hard segments. Instead, our results indicate that the amorphous phase is microphase separated into a highly mobile PTMO-rich phase and a PBT/PTMO mixed phase. This effect is most pronounced in copoly(ether esters) with a relatively large concentration of soft segments and relatively long soft segment block lengths. We stress that our structural model for copoly(ether esters) can only be formulated due to the application of various analytical techniques. One technique by itself cannot provide the complete picture. The model gives a better insight into how the chemical structure and composition of copoly(ether esters) influence the microstructure which controls the end-use properties. This better understanding in structure−property relationships is a powerful tool for designing materials with the desired properties and performance.

Acknowledgment. We thank Monique Walet and Yvonne Engelen for the TEM studies, Thijs Pijpers for performing the DSC experiments, and Jos Linsen for the DMTA experiments. Carmen Alves is gratefully acknowledged for performing the infrared experiments.

References and Notes

(1) Adams, R. K.; Hoeschele, G. K.; Witsiepe, W. K. *Thermoplastic Elastomers*, 2nd ed.; Holden, G., Legge, N. R., Quirk, R., Schroeder, H. E., Eds.; Hanser Publishers: Munich, 1996; p 191.
(2) Miller, J. A.; McKenna, J. M.; Pruckmayr, G.; Epperson, J. E.; Cooper, S. L. *Macromolecules* **1985**, *18*, 1727.
(3) Soliman, M.; Dijkstra, K.; Borggreve, R. J. M.; Wedler, W.; Winter, H. H. *Makromolekulares Kolloquium*, Freiburg, 1998.
(4) Veenstra, H.; Hoogvliet, R. M.; Norder, B.; Posthuma de Boer, A. *J. Polym. Sci. B* **1998**, *36*, 1795.
(5) Zhu, L. L.; Wegner, G.; Bandara, U. *Makromol. Chem.* **1981**, *182*, 3639.
(6) Vallance, M. A.; Cooper, S. L. *Macromolecules* **1984**, *17*, 1208.
(7) Zhu, L. L.; Wegner, G. *Makromol. Chem.* **1981**, *182*, 3625.
(8) Cella, R. J. *J. Polym. Sci., Symp.* **1973**, *42*, 727.
(9) Phillips, R. A.; McKenna, J. M.; Cooper, S. L. *J. Polym. Sci. B* **1994**, *32*, 791.
(10) Castles Stevenson, J.; Cooper, S. L. *Macromolecules* **1988**, *21*, 1309.
(11) Seymour, R. W.; Overton, J. R.; Corley, L. S. *Macromolecules* **1975**, *8*, 331.
(12) Wegner, G.; Fujii, T.; Meyer, W.; Lieser, G. *Angew. Makromol. Chem.* **1978**, *74*, 295.
(13) Cory, D. G.; Ritchey, W. M. *Macromolecules* **1989**, *22*, 1611.
(14) Min, B.; Bang, E. *Polym. J.* **1999**, *31*, 42.
(15) Fakirov, S.; Apostolov, A. A.; Boeseke, P.; Zachmann, H. G. *J. Macromol. Sci. Phys. B* **1990**, *29*, 379.
(16) Schmidt, A.; Veeman, W. S.; Litvinov V. M.; Gabriëlse, W. *Macromolecules* **1998**, *5*, 1652.
(17) It is noted that this resonance is due to the so-called "central" OCH_2 carbons of PTMO excluding the OCH_2 carbons that flank the terephthalate unit and therefore have a different chemical shift.
(18) Murmatsu, S.; Lando, J. B. *Macromolecules* **1998**, *31*, 1866.
(19) Tashiro, K.; Hiramatsu, M.; Li, T.; Masamichio, K.; Hiroyuki, T. *Sen'i Gakkaishi* **1986**, *42*, T597.

MA0012696